

Kittel
Chapter 9

Tight binding Model

Part 2

CALCULATION OF ENERGY BANDS

Few masters of energy band calculation learned their methods entirely from books. Band calculation is a craft learned by experience, often developed in groups, and needing access to computers. Wigner and Seitz, who performed the first serious band calculations in 1933, refer to afternoons spent on the manual desk calculators of those days, using one afternoon for a trial wavefunction. Modern computers have eased the pain. However, the formulation of the problem requires great care, and the computer programs are not trivial.

Here we limit ourselves to three methods useful to beginners: the tight-binding method, useful for interpolation; the Wigner-Seitz method, useful for the visualization and understanding of the alkali metals; and the pseudopotential method, utilizing the general theory of Chapter 7, which shows the simplicity of many problems. Reviews of these and other methods are cited at the end of this chapter.

Tight Binding Method for Energy Bands

Let us start with neutral separated atoms and watch the changes in the atomic energy levels as the charge distributions of adjacent atoms overlap when the atoms are brought together to form a crystal. Consider two hydrogen atoms, each with an electron in the 1s ground state. The wavefunctions ψ_A , ψ_B on the separated atoms are shown in Fig. 16a.

As the atoms are brought together, their wavefunctions overlap. We consider the two combinations $\psi_A \pm \psi_B$. Each combination shares an electron with the two protons, but an electron in the state $\psi_A + \psi_B$ will have a somewhat lower energy than in the state $\psi_A - \psi_B$.

In $\psi_A + \psi_B$ the electron spends part of the time in the region midway between the two protons, and in this region it is in the attractive potential of both protons at once, thereby increasing the binding energy. In $\psi_A - \psi_B$ the probability density vanishes midway between the nuclei; an extra binding does not appear.

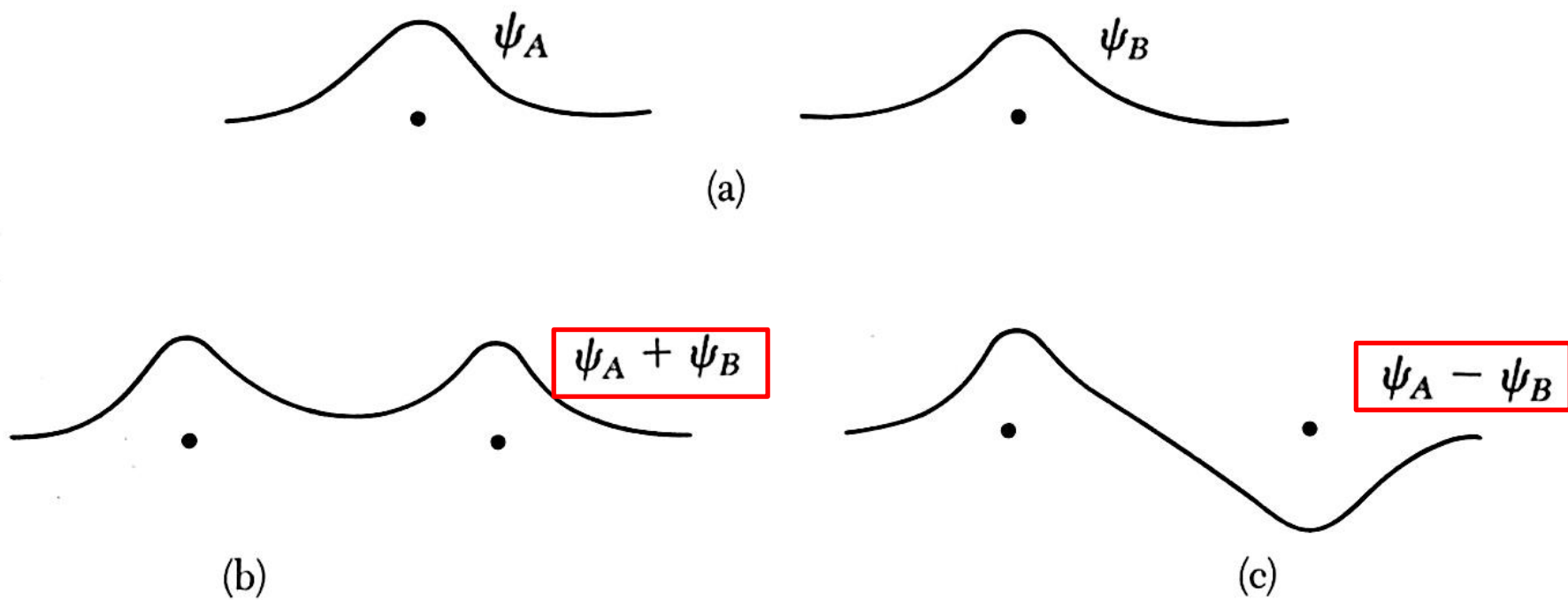


Figure 16 (a) Schematic drawing of wavefunctions of electrons on two hydrogen atoms at large separation. (b) Ground state wavefunction at closer separation. (c) Excited state wavefunction.

As two atoms are brought together, two separated energy levels are formed for each level of the isolated atom. For N atoms, N orbitals are formed for each orbital of the isolated atom (Fig. 17).

As free atoms are brought together, the coulomb interaction between the atom cores and the electron splits the energy levels, spreading them into bands. Each state of given quantum number of the free atom is spread in the crystal into a band of energies. The width of the band is proportional to the strength of the overlap interaction between neighboring atoms.

There will be bands formed from p, d, \dots states ($l = 1, 2, \dots$) of the free atoms. States degenerate in the free atom will form different bands. Each will not have the same energy as any other band over any substantial range of the wavevector. Bands may coincide in energy at certain values of \mathbf{k} in the Brillouin zone.

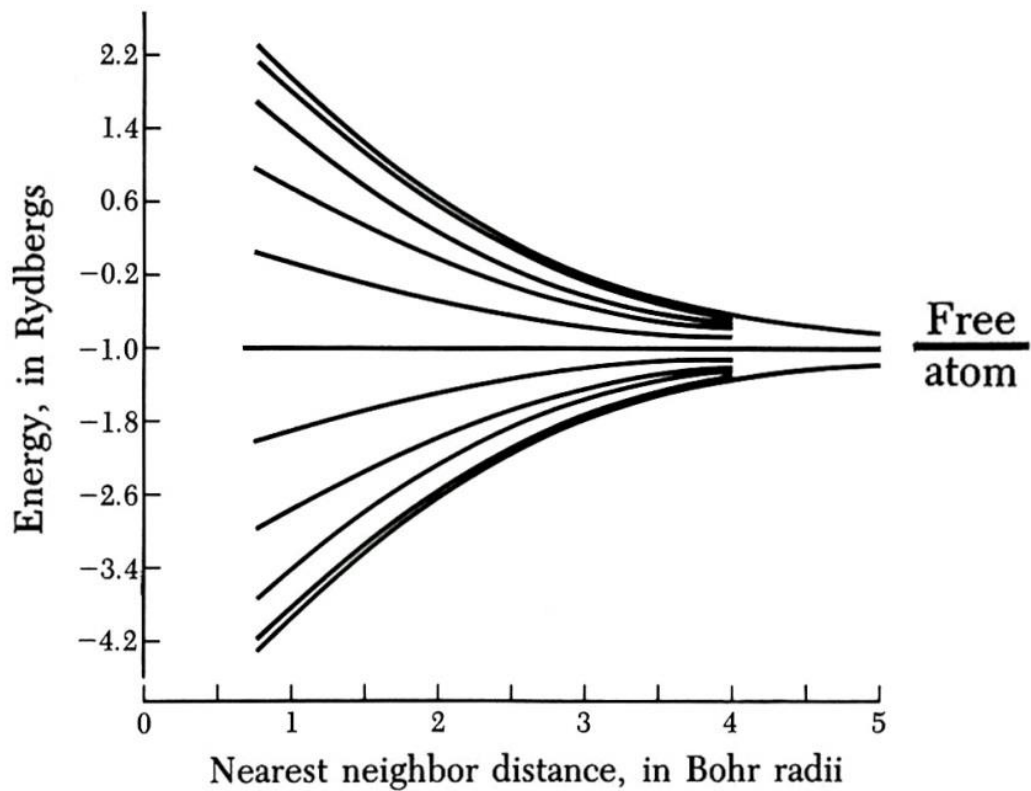


Figure 17 The 1s band of a ring of 20 hydrogen atoms; the one-electron energy calculated in the tight-binding approximation with the nearest-neighbor overlap integral of Eq. (9).

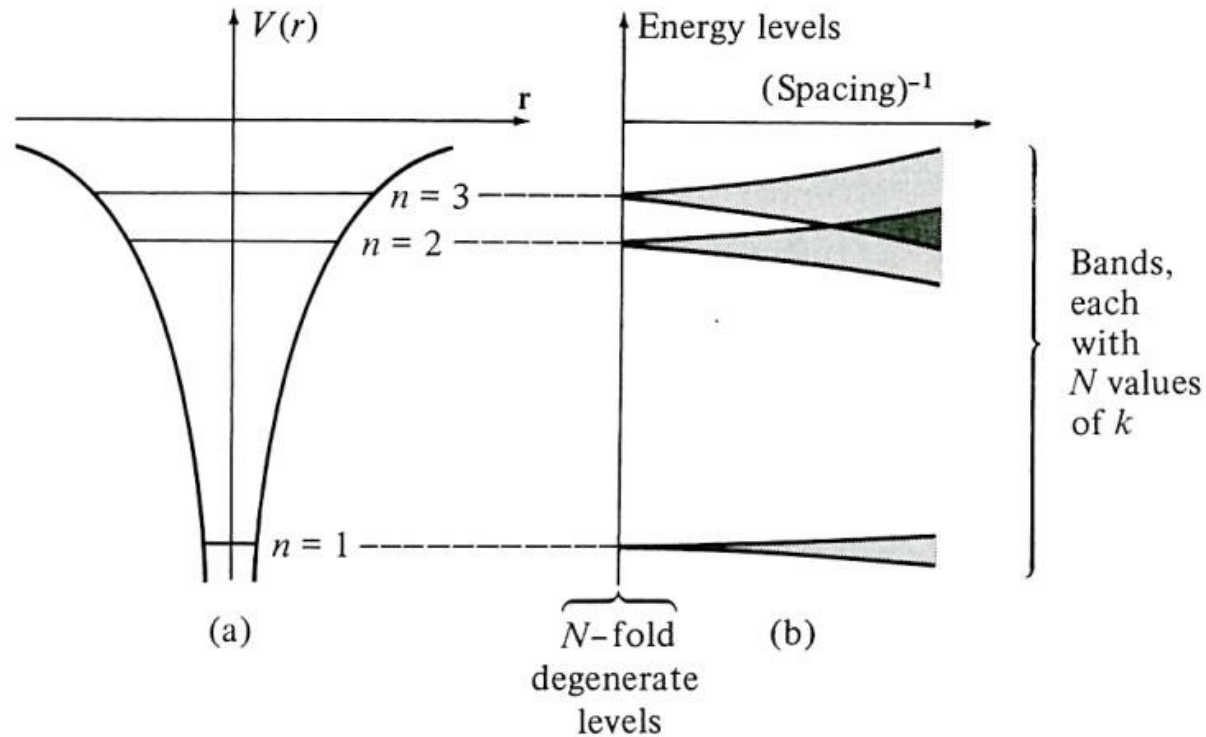


Figure 10.4

Atoms far apart ----- atoms closer

(a) Schematic representation of nondegenerate electronic levels in an atomic potential. (b) The energy levels for N such atoms in a periodic array, plotted as a function of mean inverse interatomic spacing. When the atoms are far apart (small overlap integrals) the levels are nearly degenerate, but when the atoms are closer together (larger overlap integrals), the levels broaden into bands.

The approximation that starts out from the wavefunctions of the free atoms is known as the tight binding approximation or the LCAO (linear combination of atomic orbitals) approximation. The approximation is quite good for the inner electrons of atoms, but it is not often a good description of the conduction electrons themselves. It is used to describe approximately the d bands of the transition metals and the valence bands of diamondlike and inert gas crystals.

Suppose that the ground state of an electron moving in the potential $U(\mathbf{r})$ of an isolated atom is $\varphi(\mathbf{r})$, an s state. The treatment of bands arising from degenerate (p, d, \dots) atomic levels is more complicated. If the influence of one atom on another is small, we obtain an approximate wavefunction for one electron in the whole crystal by taking

$$\psi_{\mathbf{k}}(\mathbf{r}) = \sum_j C_{\mathbf{k}j} \varphi(\mathbf{r} - \mathbf{r}_j) , \quad (4)$$

where the sum is over all lattice points. We assume the primitive basis contains one atom. This function is of the Bloch form (7.7) if $C_{\mathbf{k}j} = N^{-1/2} e^{i\mathbf{k} \cdot \mathbf{r}_j}$, which gives, for a crystal of N atoms,

$$\psi_{\mathbf{k}}(\mathbf{r}) = N^{-1/2} \sum_j \exp(i\mathbf{k} \cdot \mathbf{r}_j) \varphi(\mathbf{r} - \mathbf{r}_j) . \quad (5)$$

We prove (5) is of the Bloch form. Consider a translation \mathbf{T} connecting two lattice points:

$$\begin{aligned}
 \psi_{\mathbf{k}}(\mathbf{r} + \mathbf{T}) &= N^{-1/2} \sum_j \exp(i\mathbf{k} \cdot \mathbf{r}_j) \varphi(\mathbf{r} + \mathbf{T} - \mathbf{r}_j) \\
 &= \exp(i\mathbf{k} \cdot \mathbf{T}) N^{-1/2} \sum_j \exp[i\mathbf{k} \cdot (\mathbf{r}_j - \mathbf{T})] \varphi[\mathbf{r} - (\mathbf{r}_j - \mathbf{T})] \quad (6) \\
 &= \exp(i\mathbf{k} \cdot \mathbf{T}) \psi_{\mathbf{k}}(\mathbf{r}) ,
 \end{aligned}$$

exactly the Bloch condition.

We find the first-order energy by calculating the diagonal matrix elements of the hamiltonian of the crystal:

$$\langle \mathbf{k} | H | \mathbf{k} \rangle = N^{-1} \sum_j \sum_m \exp[i\mathbf{k} \cdot (\mathbf{r}_j - \mathbf{r}_m)] \langle \varphi_m | H | \varphi_j \rangle , \quad (7)$$

where $\varphi_m \equiv \varphi(\mathbf{r} - \mathbf{r}_m)$. Writing $\boldsymbol{\rho}_m = \mathbf{r}_m - \mathbf{r}_j$,

$$\langle \mathbf{k} | H | \mathbf{k} \rangle = \sum_m \exp(-i\mathbf{k} \cdot \boldsymbol{\rho}_m) \int dV \varphi^*(\mathbf{r} - \boldsymbol{\rho}_m) H \varphi(\mathbf{r}) . \quad (8)$$

We now neglect all integrals in (8) except those on the same atom and those between nearest neighbors connected by $\boldsymbol{\rho}$. We write

$$\int dV \varphi^*(\mathbf{r})H\varphi(\mathbf{r}) = -\alpha ; \quad \int dV \varphi^*(\mathbf{r} - \boldsymbol{\rho})H\varphi(\mathbf{r}) = -\gamma ; \quad (9)$$

and we have the first-order energy, provided $\langle \mathbf{k} | \mathbf{k} \rangle = 1$:

$$\langle \mathbf{k} | H | \mathbf{k} \rangle = -\alpha - \gamma \sum_m \exp(-i\mathbf{k} \cdot \boldsymbol{\rho}_m) = \epsilon_{\mathbf{k}} . \quad (10)$$

The dependence of the overlap energy γ on the interatomic separation ρ can be evaluated explicitly for two hydrogen atoms in 1s states. In rydberg energy units, $\text{Ry} = me^4/2\hbar^2$, we have

$$\gamma(\text{Ry}) = 2(1 + \rho/a_0) \exp(-\rho/a_0) , \quad (11)$$

where $a_0 = \hbar^2/me^2$. The overlap energy decreases exponentially with the separation.

For a simple cubic structure the nearest-neighbor atoms are at

$$\boldsymbol{\rho}_m = (\pm a, 0, 0) ; (0, \pm a, 0) ; (0, 0, \pm a) , \quad (12)$$

so that (10) becomes

$$\epsilon_{\mathbf{k}} = -\alpha - 2\gamma(\cos k_x a + \cos k_y a + \cos k_z a) . \quad (13)$$

Thus the energies are confined to a band of width 12γ . The weaker the overlap, the narrower is the energy band. A constant energy surface is shown in Fig. 15. For $ka \ll 1$, $\epsilon_{\mathbf{k}} \simeq -\alpha - 6\gamma + \gamma k^2 a^2$. The effective mass is $m^* = \hbar^2/2\gamma a^2$. When the overlap integral γ is small, the band is narrow and the effective mass is high.

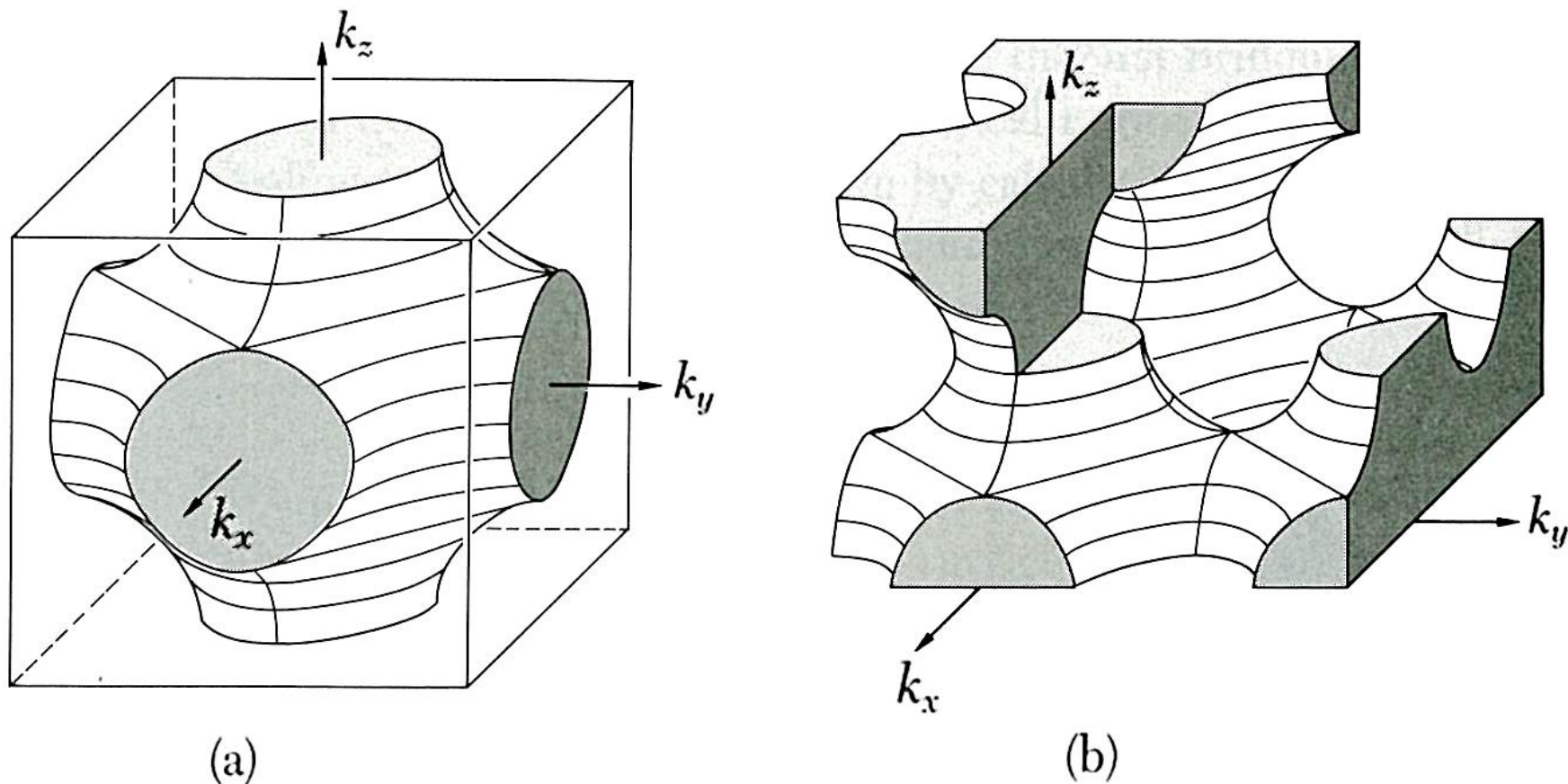


Figure 15 Constant energy surface in the Brillouin zone of a simple cubic lattice, for the assumed energy band $\epsilon_k = -\alpha - 2\gamma(\cos k_x a + \cos k_y a + \cos k_z a)$. (a) Constant energy surface $\epsilon = -\alpha$. The filled volume contains one electron per primitive cell. (b) The same surface exhibited in the periodic zone scheme. The connectivity of the orbits is clearly shown. Can you find electron, hole, and open orbits for motion in a magnetic field $B\hat{z}$? (A. Sommerfeld and H. A. Bethe.)

We considered one orbital of each free atom and obtained one band $\epsilon_{\mathbf{k}}$. The number of orbitals in the band that corresponds to a nondegenerate atomic level is $2N$, for N atoms. We see this directly: values of \mathbf{k} within the first Brillouin zone define independent wavefunctions. The simple cubic zone has $-\pi/a < k_x < \pi/a$, etc. The zone volume is $8\pi^3/a^3$. The number of orbitals (counting both spin orientations) per unit volume of \mathbf{k} space is $V/4\pi^3$, so that the number of orbitals is $2V/a^3$. Here V is the volume of the crystal, and $1/a^3$ is the number of atoms per unit volume. Thus there are $2N$ orbitals.

For the bcc structure with eight nearest neighbors,

$$\epsilon_{\mathbf{k}} = -\alpha - 8\gamma \cos \frac{1}{2}k_x a \cos \frac{1}{2}k_y a \cos \frac{1}{2}k_z a . \quad (14)$$

For the fcc structure with 12 nearest neighbors,

$$\epsilon_{\mathbf{k}} = -\alpha - 4\gamma(\cos \frac{1}{2}k_y a \cos \frac{1}{2}k_z a + \cos \frac{1}{2}k_z a \cos \frac{1}{2}k_x a + \cos \frac{1}{2}k_x a \cos \frac{1}{2}k_y a) . \quad (15)$$

A constant energy surface is shown in Fig. 18.

fcc

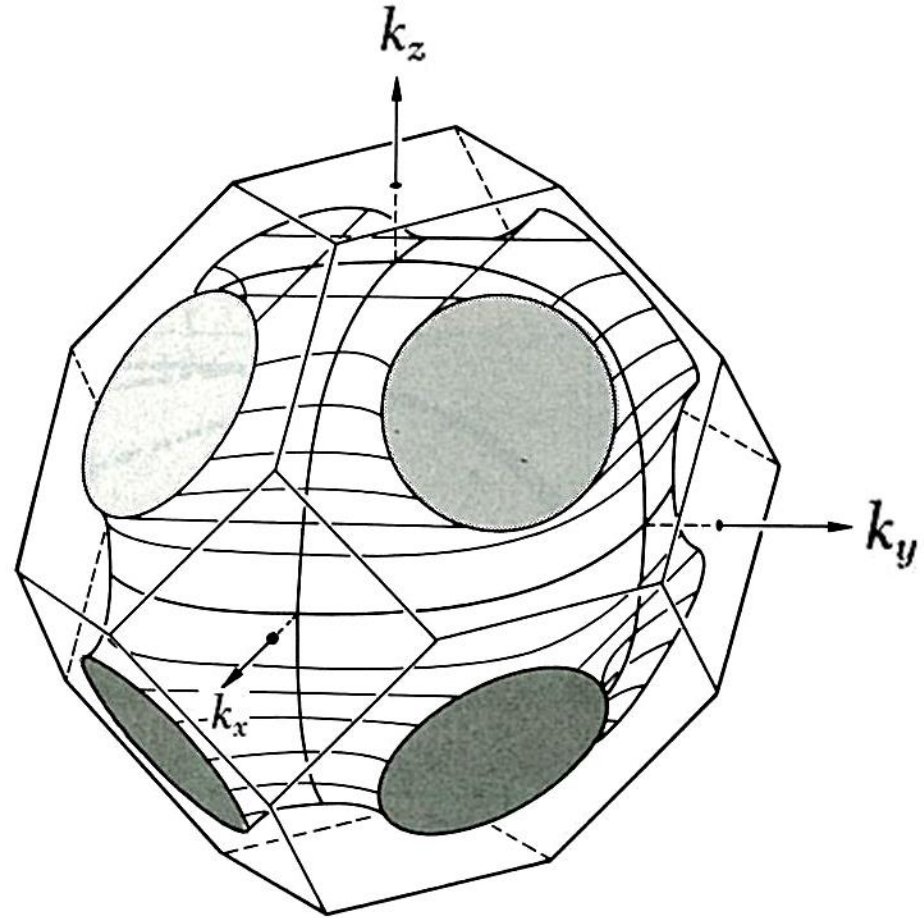


Figure 18 A constant energy surface of an fcc crystal structure, in the nearest-neighbor tight-binding approximation. The surface shown has $\epsilon = -\alpha + 2|\gamma|$.

Ashcoft Mermin

Chapter 11

on

Tight binding Model

The coefficients (10.16) to (10.18) may be simplified by appealing to certain symmetries. Since ϕ is an s -level, $\phi(\mathbf{r})$ is real and depends only on the magnitude r . From this it follows that $\alpha(-\mathbf{R}) = \alpha(\mathbf{R})$. This and the inversion symmetry of the Bravais lattice, which requires that $\Delta U(-\mathbf{r}) = \Delta U(\mathbf{r})$, also imply that $\gamma(-\mathbf{R}) = \gamma(\mathbf{R})$. We ignore the terms in α in the denominator of (10.15), since they give small corrections to the numerator. A final simplification comes from assuming that only nearest-neighbor separations give appreciable overlap integrals.

Putting these observations together, we may simplify (10.15) to

$$\varepsilon(\mathbf{k}) = E_s - \beta - \sum_{\text{n.n.}} \gamma(\mathbf{R}) \cos \mathbf{k} \cdot \mathbf{R}, \quad (10.19)$$

where the sum runs only over those \mathbf{R} in the Bravais lattice that connect the origin to its nearest neighbors.

To be explicit, let us apply (10.19) to a face-centered cubic crystal. The 12 nearest neighbors of the origin (see Figure 10.3) are at

$$\mathbf{R} = \frac{a}{2} (\pm 1, \pm 1, 0), \quad \frac{a}{2} (\pm 1, 0, \pm 1), \quad \frac{a}{2} (0, \pm 1, \pm 1). \quad (10.20)$$

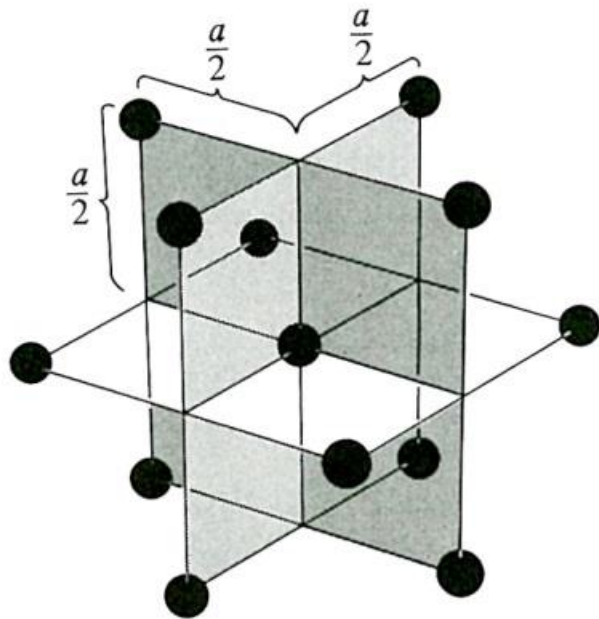


Figure 10.3

The 12 nearest neighbors of the origin in a face-centered cubic lattice with conventional cubic cell of side a .

If $\mathbf{k} = (k_x, k_y, k_z)$, then the corresponding 12 values of $\mathbf{k} \cdot \mathbf{R}$ are

$$\mathbf{k} \cdot \mathbf{R} = \frac{a}{2} (\pm k_i, \pm k_j), \quad i, j = x, y; y, z; z, x. \quad (10.21)$$

Now $\Delta U(\mathbf{r}) = \Delta U(x, y, z)$ has the full cubic symmetry of the lattice, and is therefore unchanged by permutations of its arguments or changes in their signs. This, together with the fact that the s -level wave function $\phi(\mathbf{r})$ depends only on the magnitude of \mathbf{r} , implies that $\gamma(\mathbf{R})$ is the same constant γ for all 12 of the vectors (10.20). Consequently, the sum in (10.19) gives, with the aid of (10.21),

$$\varepsilon(\mathbf{k}) = E_s - \beta - 4\gamma(\cos \frac{1}{2}k_x a \cos \frac{1}{2}k_y a + \cos \frac{1}{2}k_y a \cos \frac{1}{2}k_z a + \cos \frac{1}{2}k_z a \cos \frac{1}{2}k_x a), \quad (10.22)$$

where

$$\gamma = - \int d\mathbf{r} \phi^*(x, y, z) \Delta U(x, y, z) \phi(x - \frac{1}{2}a, y - \frac{1}{2}a, z). \quad (10.23)$$

Equation (10.22) reveals the characteristic feature of tight-binding energy bands: The bandwidth—i.e., the spread between the minimum and maximum energies in the band—is proportional to the small overlap integral γ . Thus the tight-binding bands are narrow bands, and the smaller the overlap, the narrower the band. In the limit of vanishing overlap the bandwidth also vanishes, and the band becomes N -fold degenerate, corresponding to the extreme case in which the electron simply resides on any one of the N isolated atoms. The dependence of bandwidth on overlap integral is illustrated in Figure 10.4.

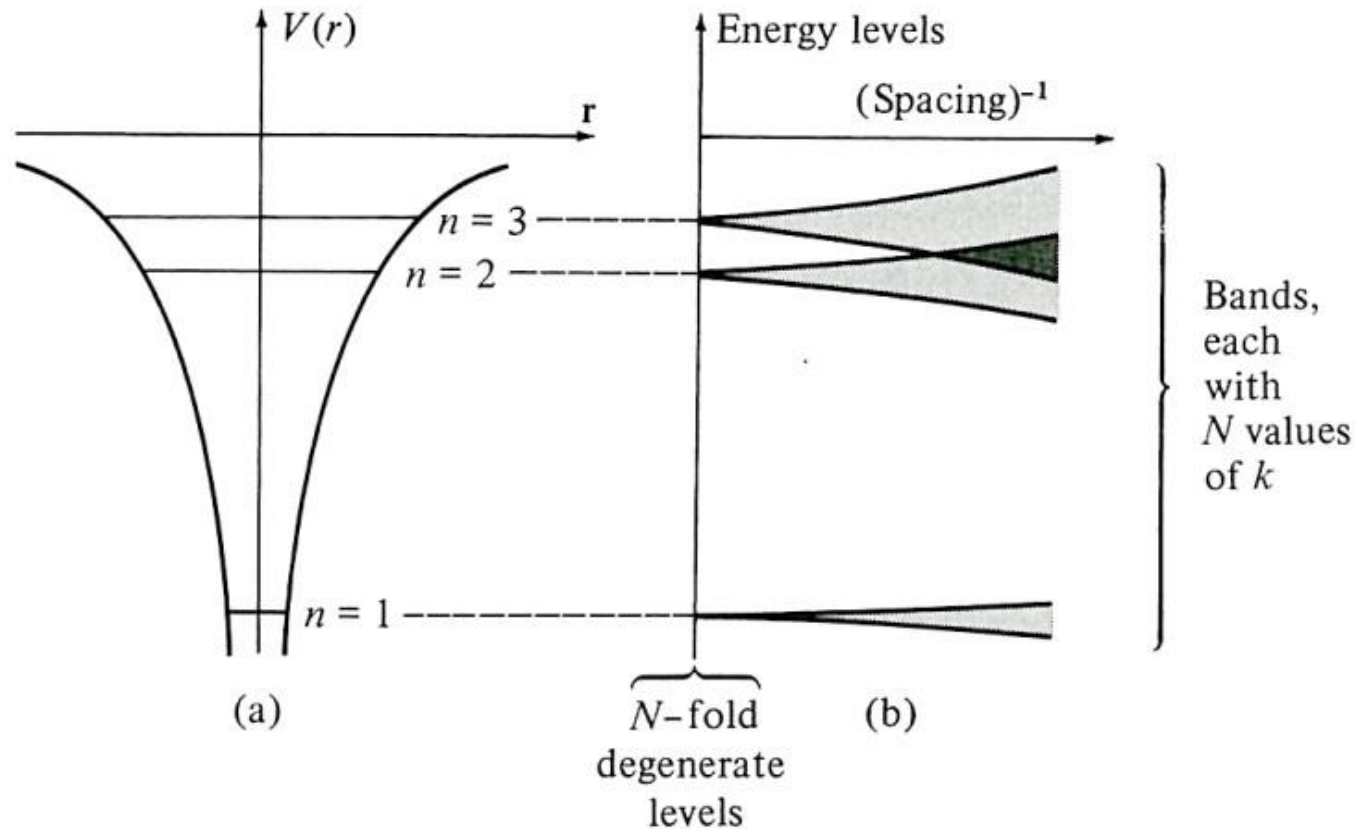


Figure 10.4

(a) Schematic representation of nondegenerate electronic levels in an atomic potential. (b) The energy levels for N such atoms in a periodic array, plotted as a function of mean inverse interatomic spacing. When the atoms are far apart (small overlap integrals) the levels are nearly degenerate, but when the atoms are closer together (larger overlap integrals), the levels broaden into bands.

In addition to displaying the effect of overlap on bandwidth, Eq. (10.22) illustrates several general features of the band structure of a face-centered cubic crystal that are not peculiar to the tight-binding case. Typical of these are the following:

1. In the limit of small ka , (10.22) reduces to:

$$\varepsilon(\mathbf{k}) = E_s - \beta - 12\gamma + \gamma k^2 a^2. \quad (10.24)$$

This is independent of the direction of \mathbf{k} —i.e., the constant-energy surfaces in the neighbourhood of $\mathbf{k} = \mathbf{0}$ are spherical.¹⁰

2. If ε is plotted along any line perpendicular to one of the square faces of the first Brillouin zone (Figure 10.5), it will cross the square face with vanishing slope (Problem 1).

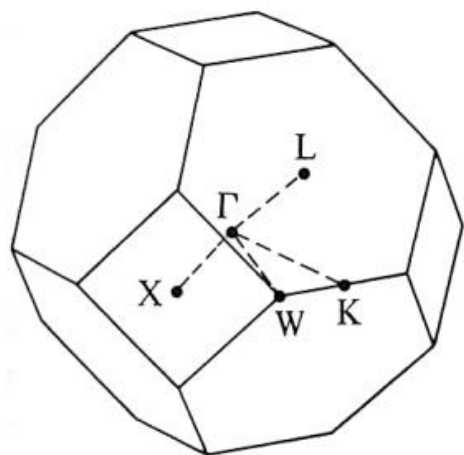


Figure 10.5

The first Brillouin zone for face-centered cubic crystals. The point Γ is at the center of the zone. The names K, L, W, and X are widely used for the points of high symmetry on the zone boundary.

3. If ε is plotted along any line perpendicular to one of the hexagonal faces of the first Brillouin zone (Figure 10.5), it need not, in general, cross the face with vanishing slope (Problem 1).¹¹

If the γ_{ij} are small, then the bandwidth is correspondingly small. As a rule of thumb, when the energy of a given atomic level increases (i.e., the binding energy decreases) so does the spatial extent of its wave function. Correspondingly, the low-lying bands in a solid are very narrow, but bandwidths increase with mean band energy. In metals the highest band (or bands) are very broad, since the spatial ranges of the highest atomic levels are comparable to a lattice constant, and the tight-binding approximation is then of doubtful validity.

3. Although the tight-binding wave function (10.6) is constructed out of localized atomic levels ϕ , an electron in a tight-binding level will be found, with equal probability, in any cell of the crystal, since its wave function (like any Bloch wave function) changes only by the phase factor $e^{ik \cdot \mathbf{R}}$ as one moves from one cell to another a distance \mathbf{R} away. Thus as \mathbf{r} varies from cell to cell, there is superimposed on the atomic structure within each cell a sinusoidal variation in the amplitudes of $\text{Re } \psi$ and $\text{Im } \psi$, as illustrated in Figure 10.7.

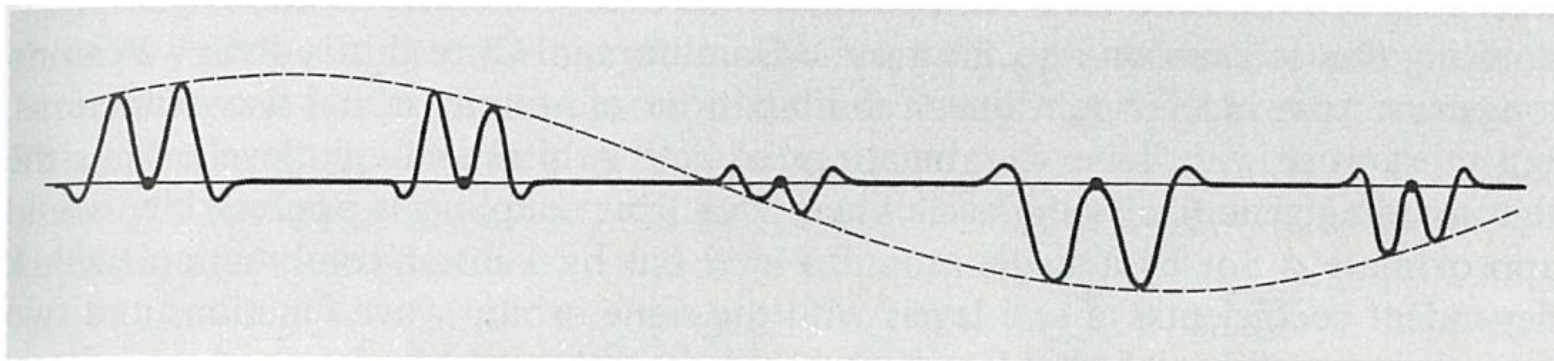


Figure 10.7

Characteristic spatial variation of the real (or imaginary) part of the tight-binding wave function (10.6).

GENERAL REMARKS ON THE TIGHT-BINDING METHOD

1. In cases of practical interest more than one atomic level appears in the expansion (10.7), leading to a 3×3 secular problem in the case of three p -levels, a 5×5 secular problem for five d -levels, etc. Figure 10.6, for example, shows the band structure that emerges from a tight-binding calculation based on the 5-fold degenerate atomic 3- d levels in nickel. The bands are plotted for three directions of symmetry in the zone, each of which has its characteristic set of degeneracies.¹²

2. A quite general feature of the tight-binding method is the relation between bandwidth and the overlap integrals

$$\gamma_{ij}(\mathbf{R}) = - \int d\mathbf{r} \phi_i^*(\mathbf{r}) \Delta U(\mathbf{r}) \phi_j(\mathbf{r} - \mathbf{R}). \quad (10.25)$$

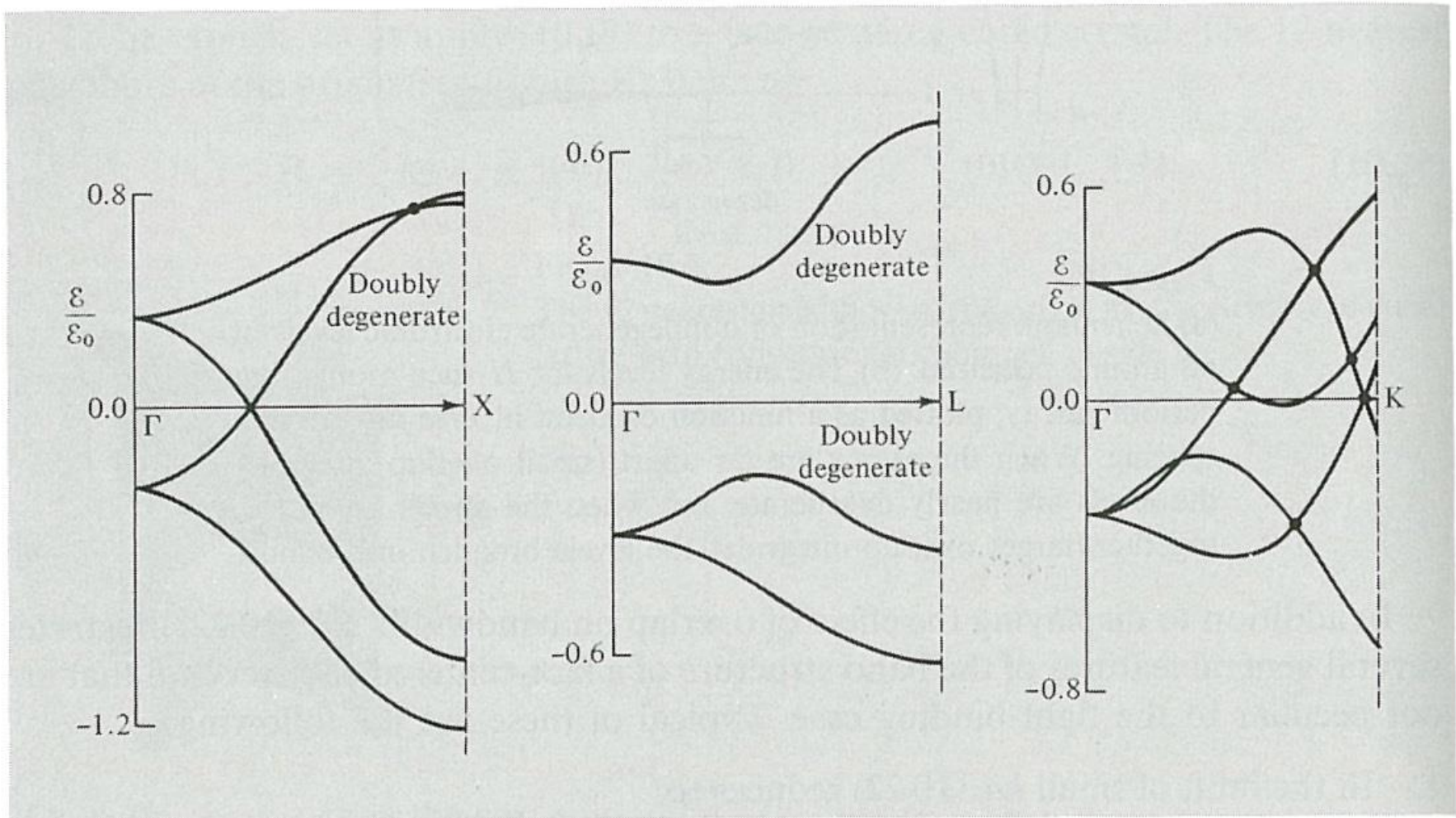


Figure 10.6

A tight-binding calculation of the 3d bands of nickel. (G. C. Fletcher, *Proc. Phys. Soc.* **A65**, 192 (1952).) Energies are given in units of $\epsilon_0 = 1.349$ eV, so the bands are about 2.7 volts wide. The lines along which ϵ is plotted are shown in Figure 10.5. Note the characteristic degeneracies along ΓX and ΓL , and the absence of degeneracy along ΓK . The great width of the bands indicates the inadequacy of so elementary a treatment.